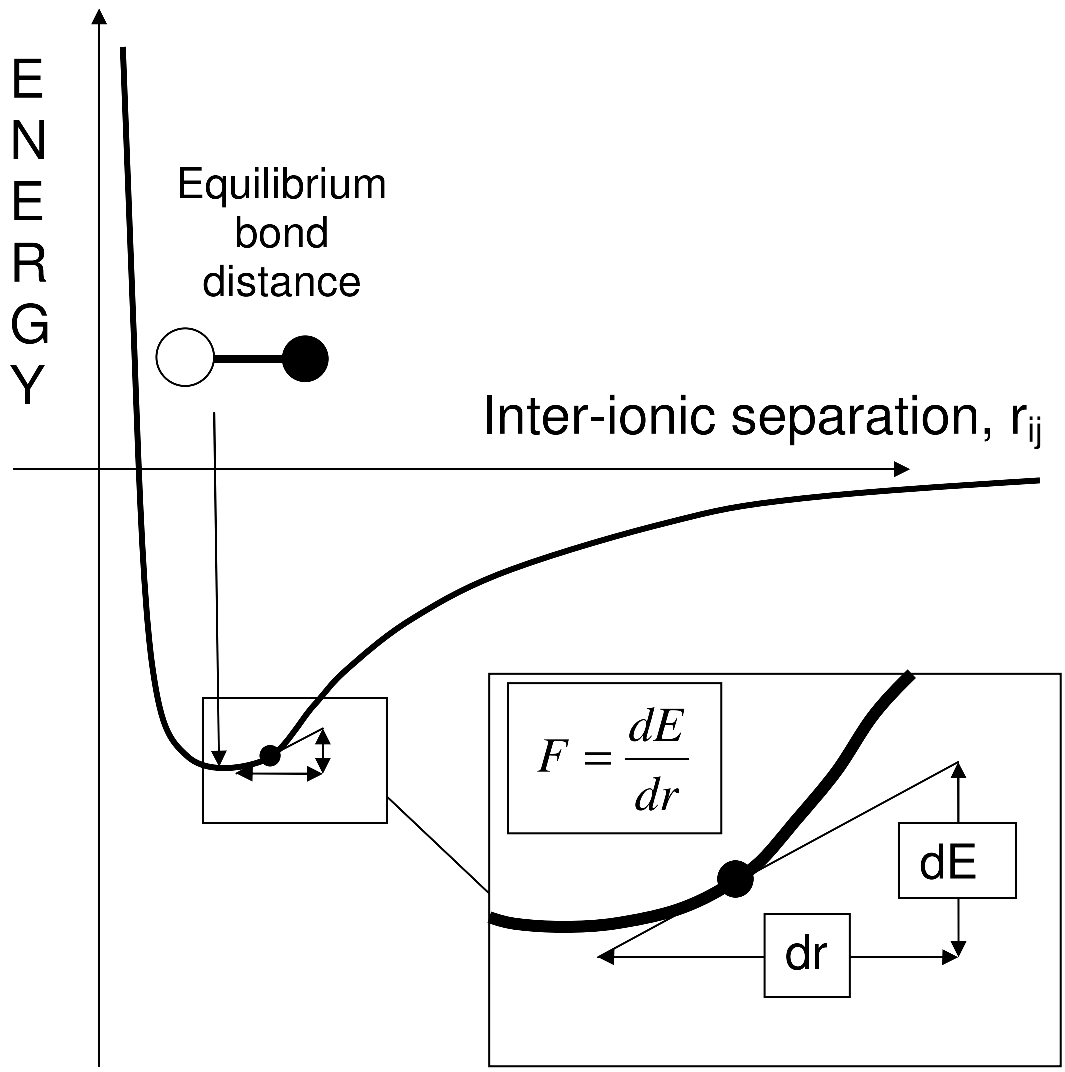
E
N
E
R
G
Y
Equilibrium
bond
distance
Inter-ionic separation, r_{ij}
$F = \frac{dE}{dr}$
dE
dr

Fig. 9.1

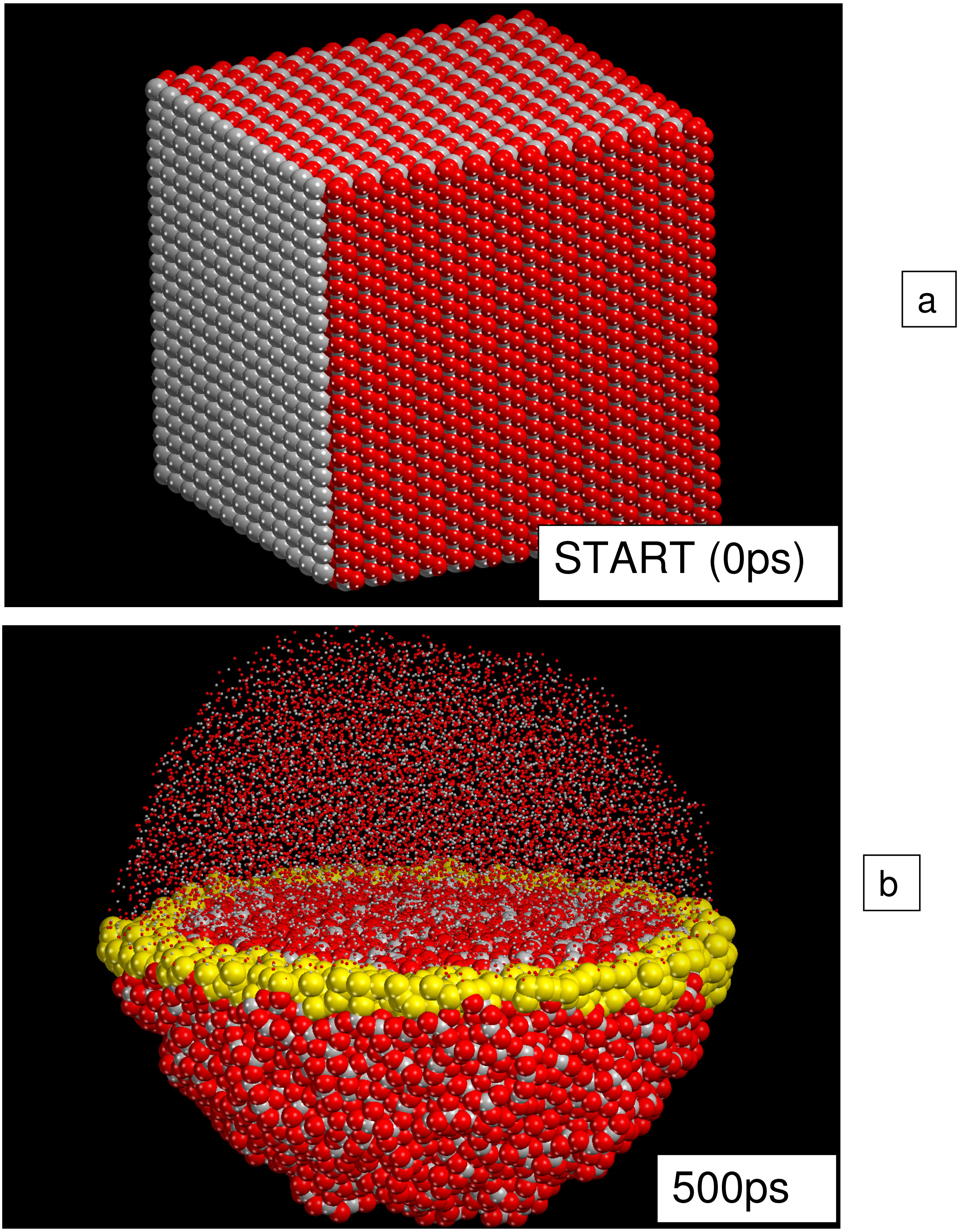

Fig. 9.2

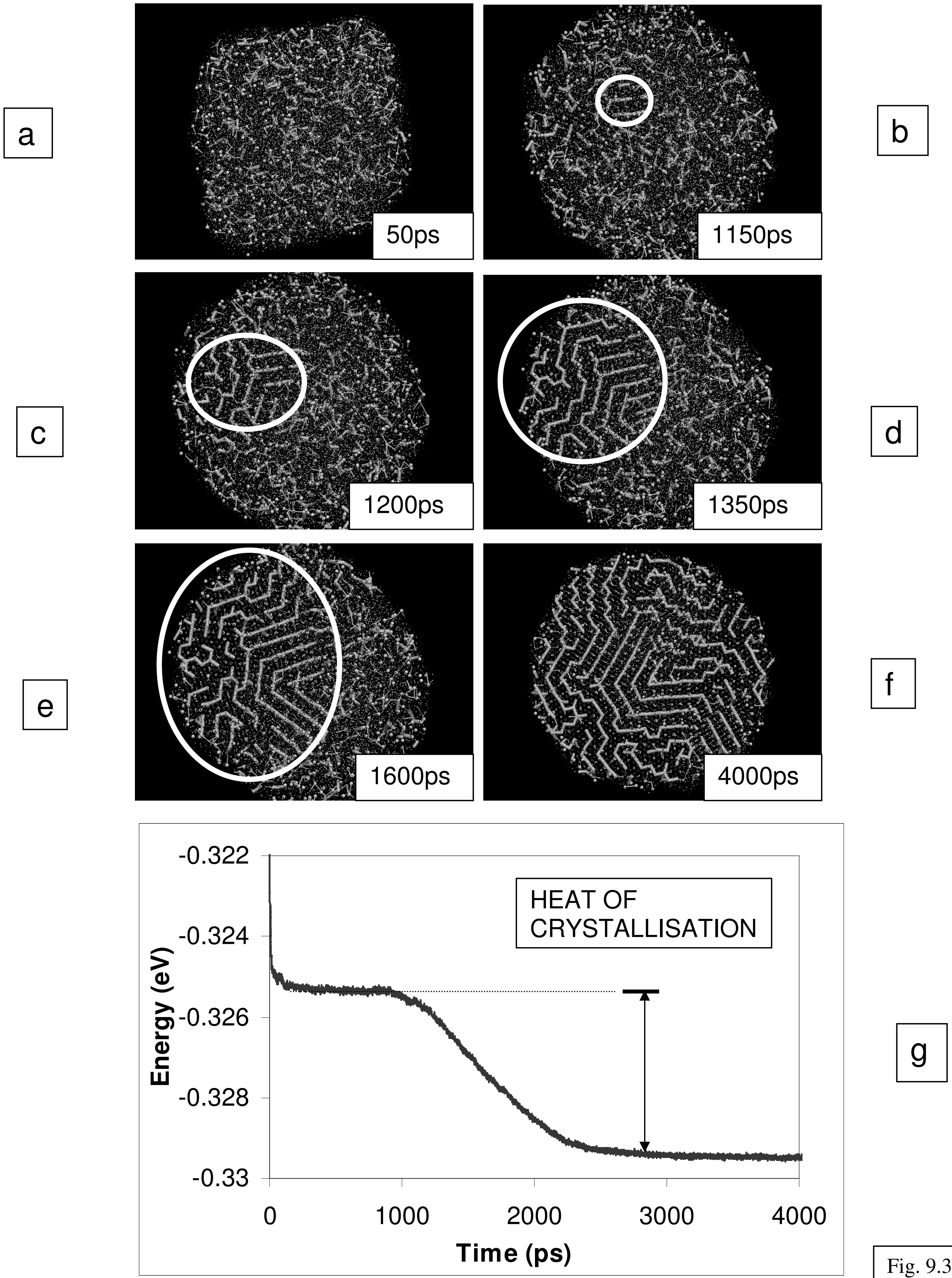
a
50ps
b
1150ps
c
1200ps
d
1350ps
e
1600ps
f
4000ps
g
HEAT OF CRYSTALLISATION
Energy (eV)
-0.322
-0.324
-0.326
-0.328
-0.33
Time (ps)
0
1000
2000
3000
4000

Fig. 9.3

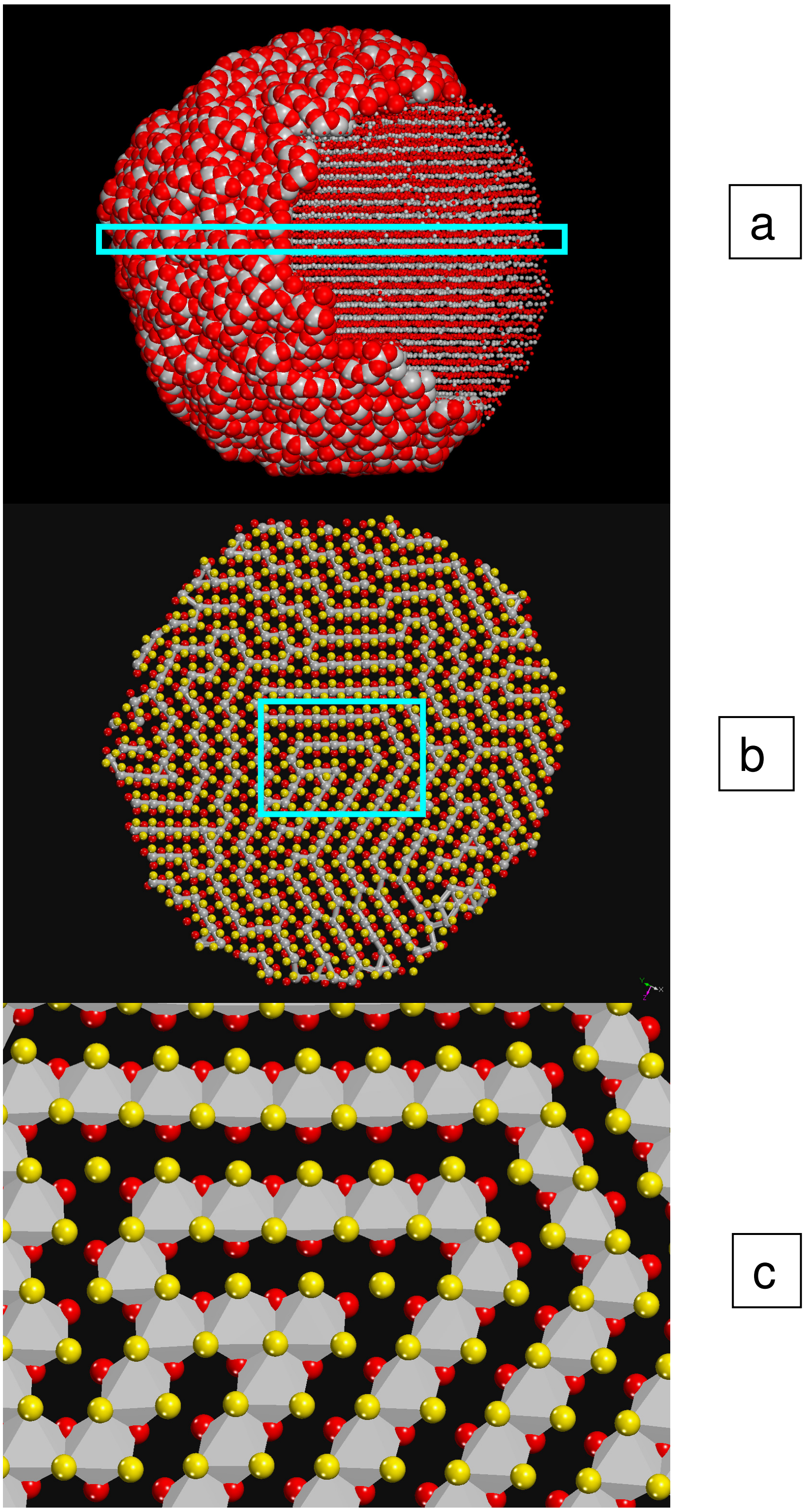

Fig. 9.4

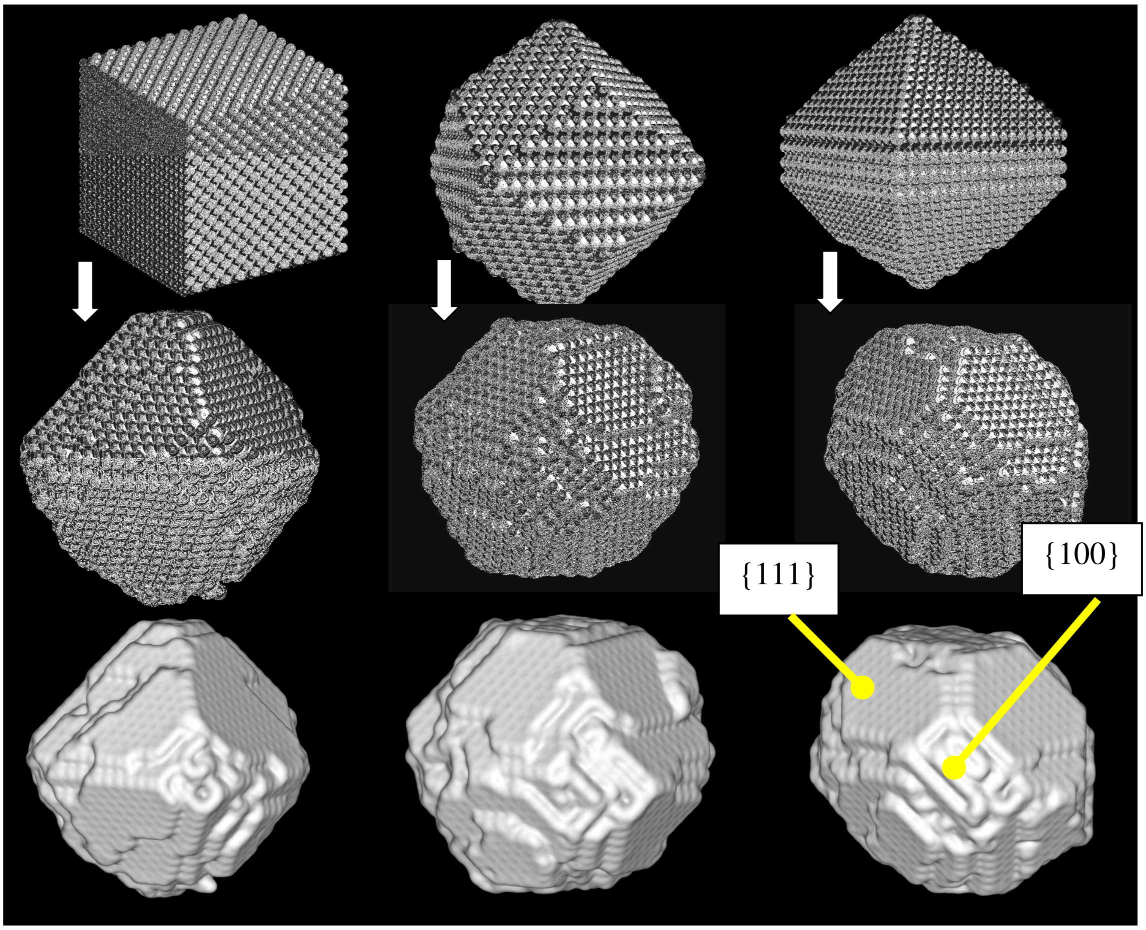

a

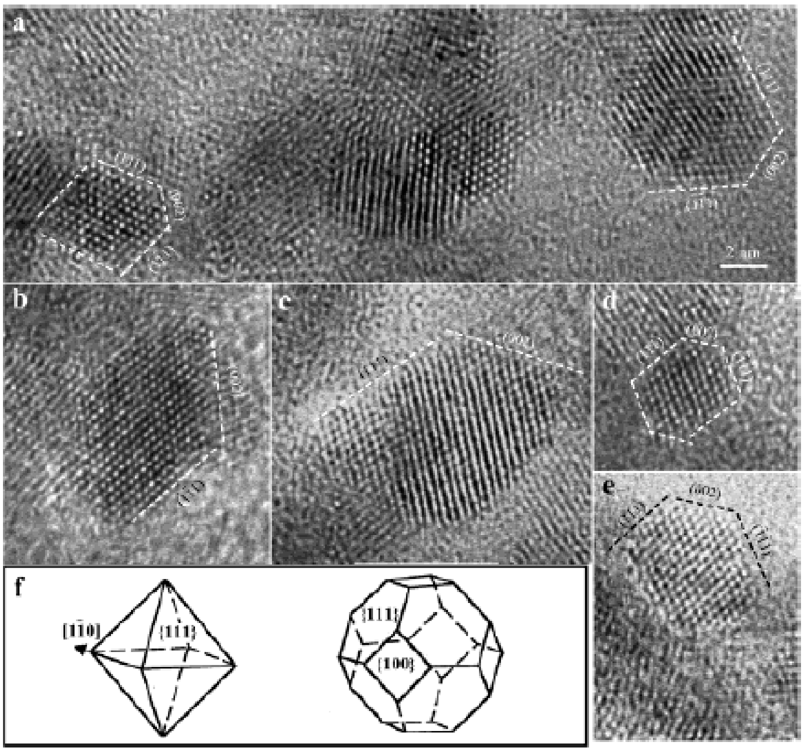

b

Fig. 9.5

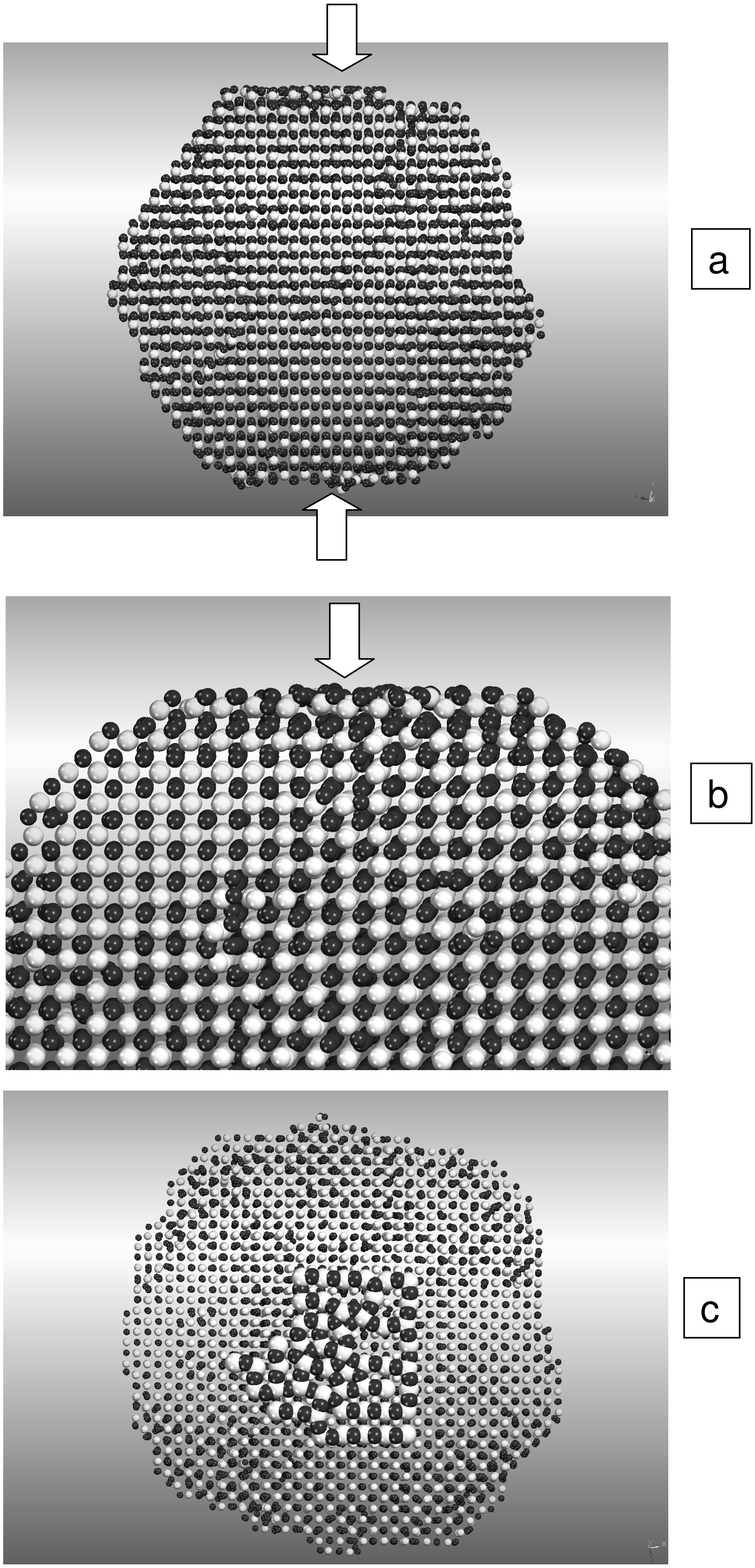

Fig. 9.6

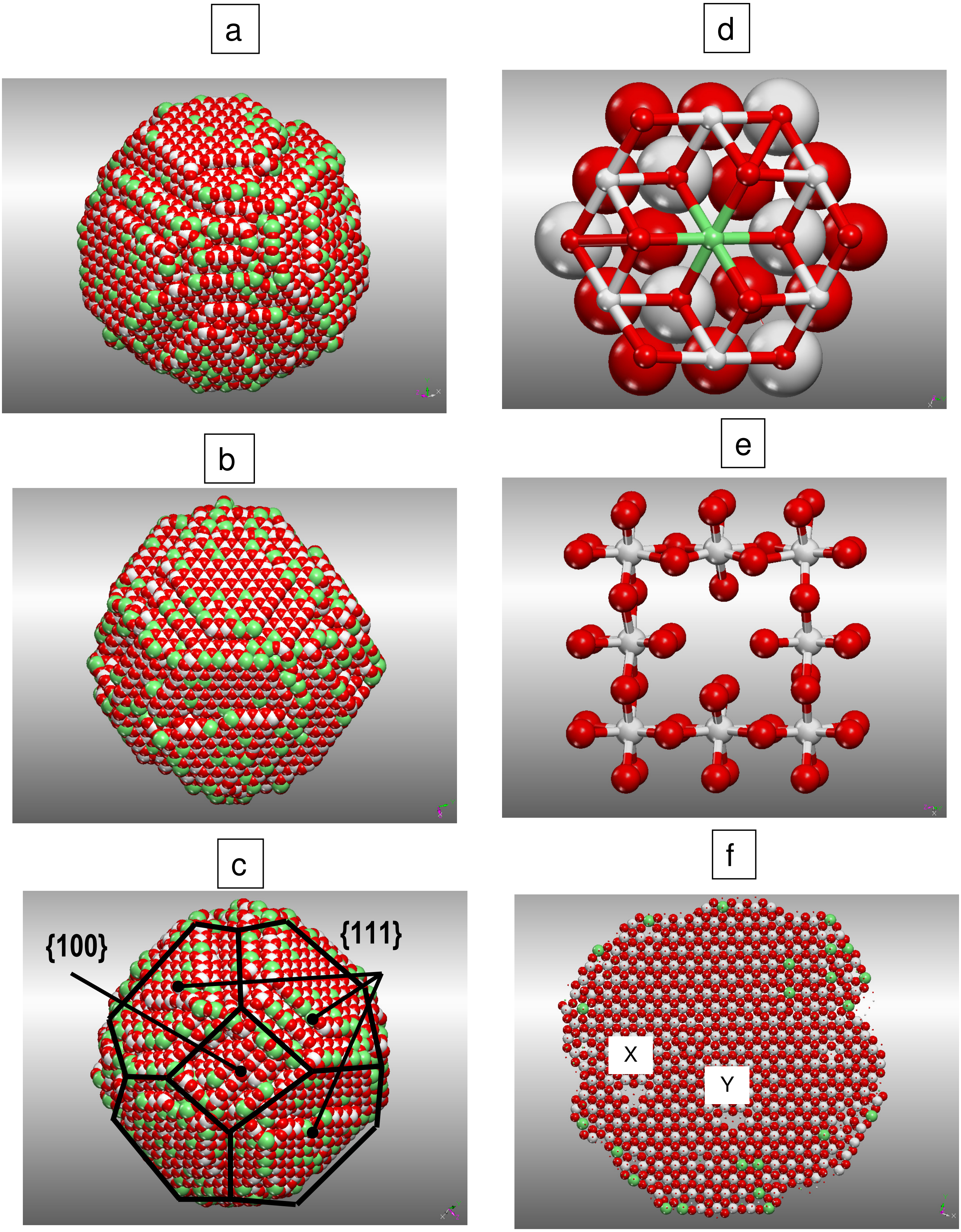

Fig. 9.7

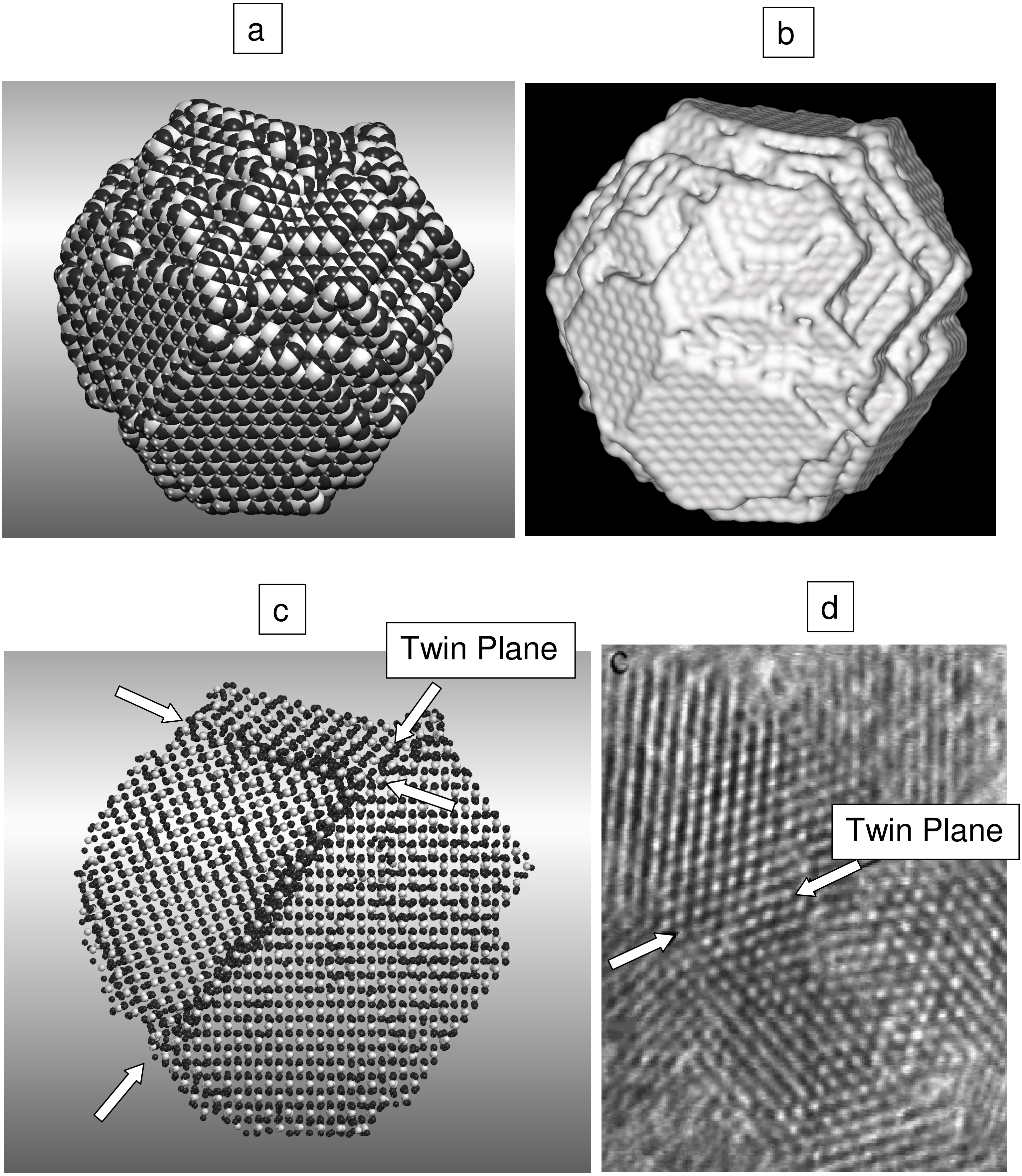

Fig. 9.8

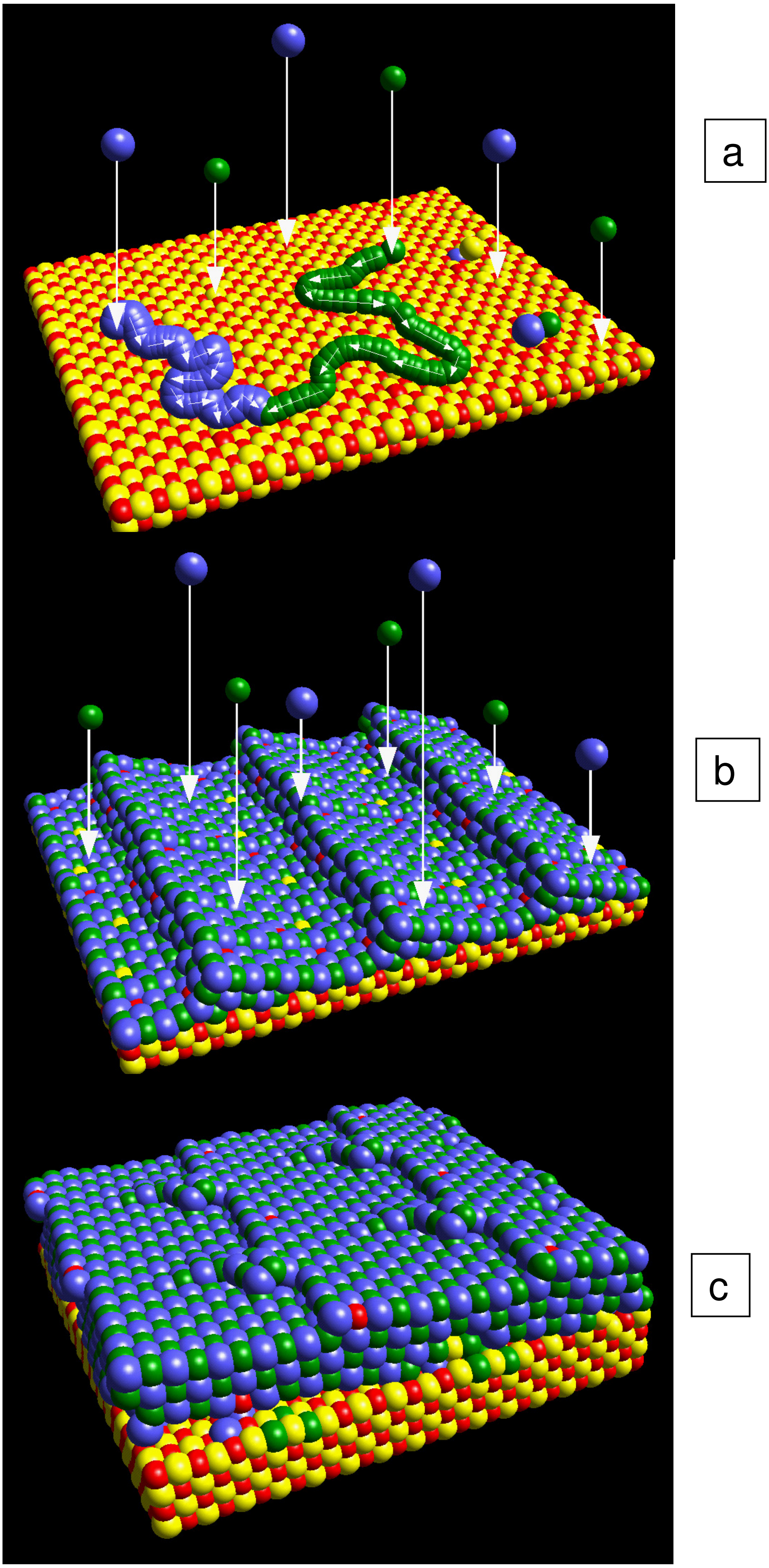

Fig. 9.9

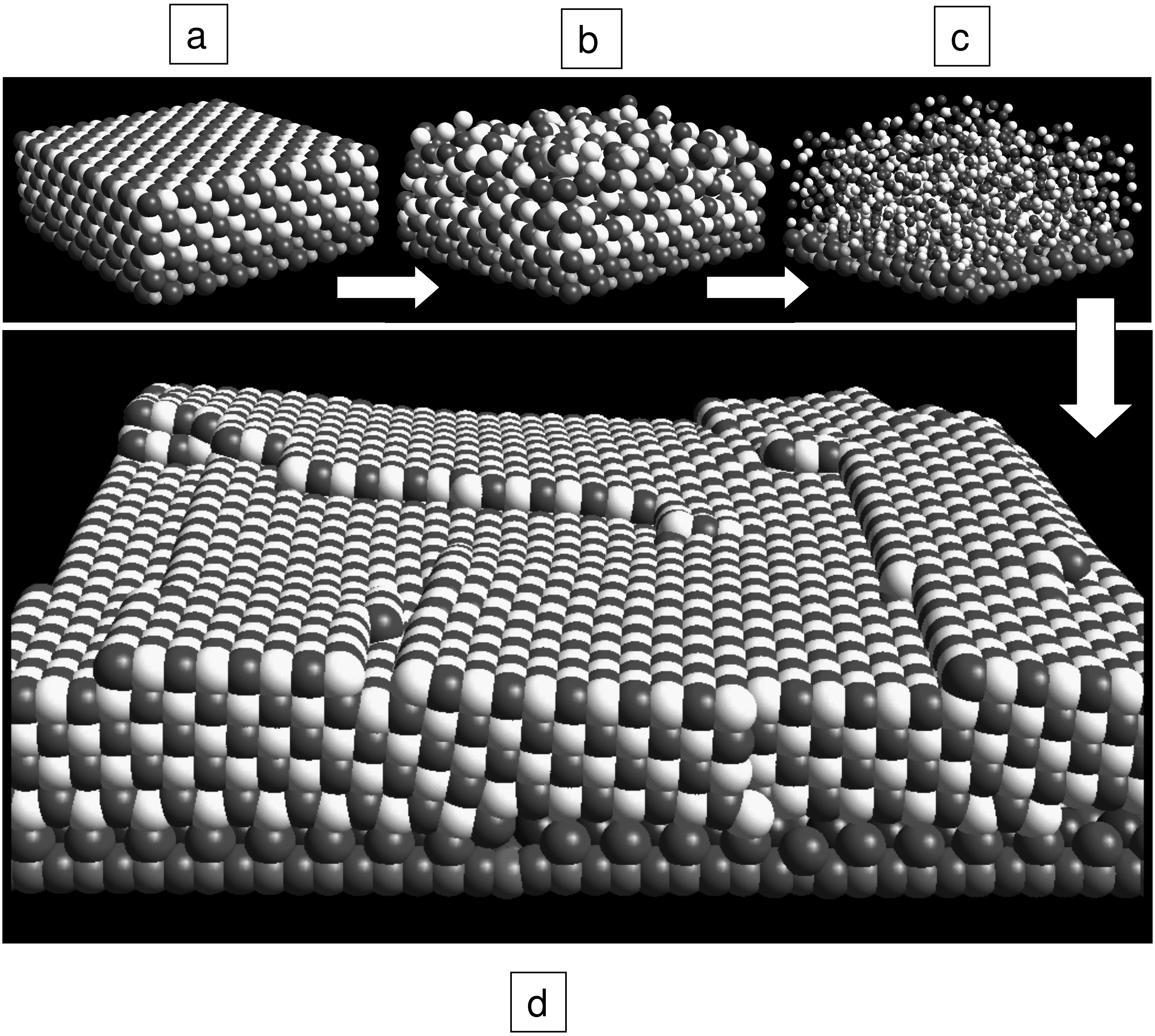

Fig. 9.10

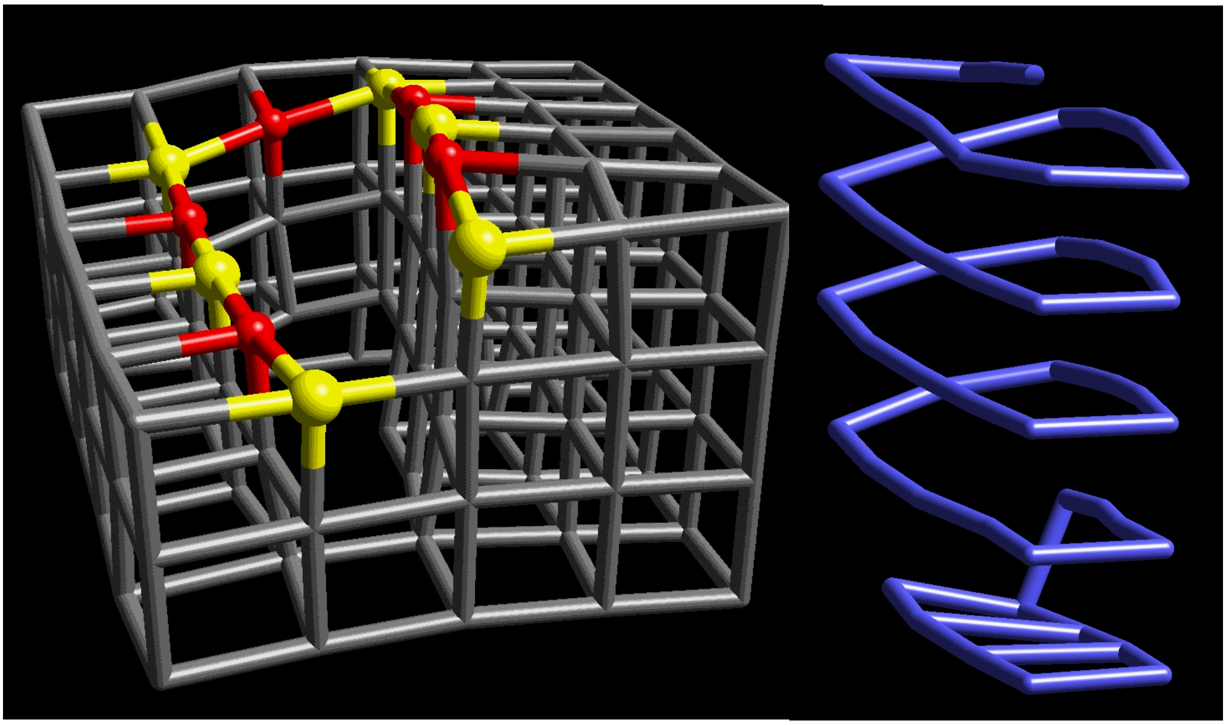

a

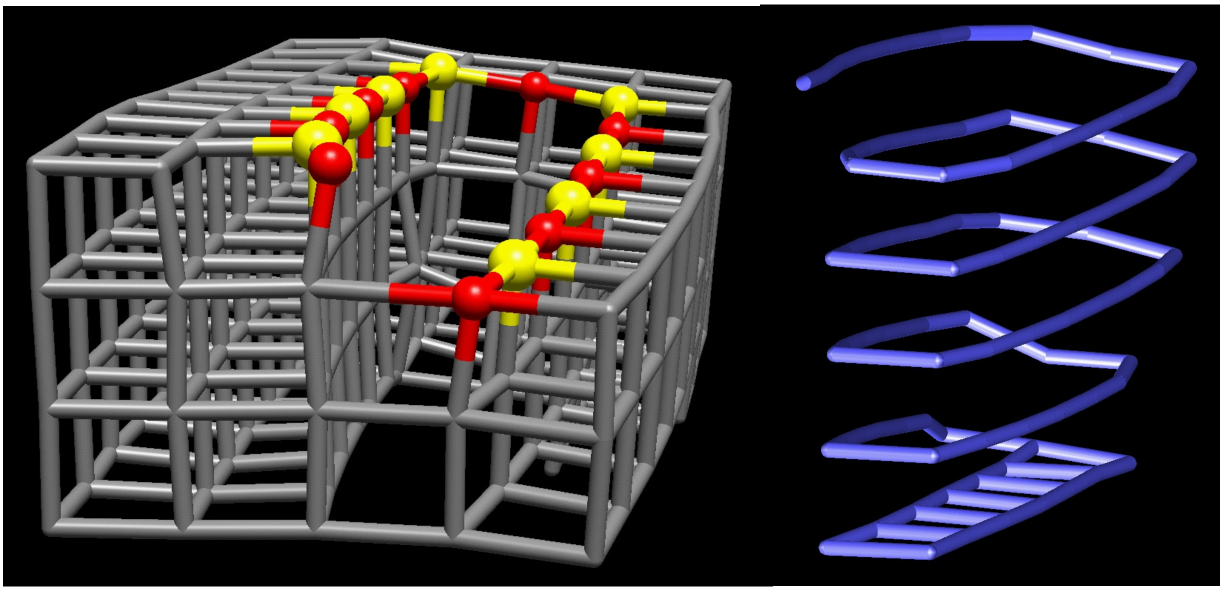

b

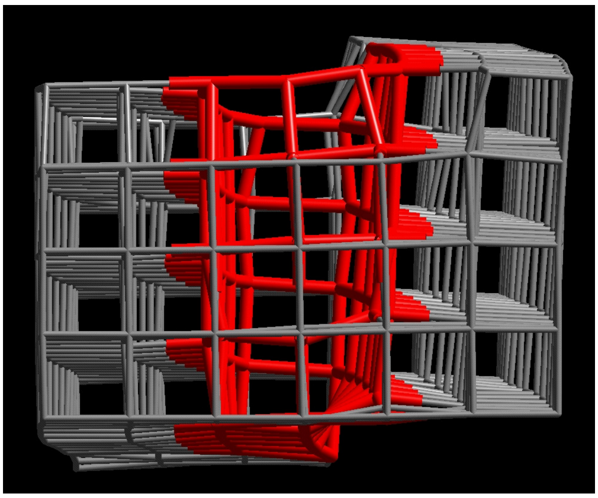

c

Fig. 9.11

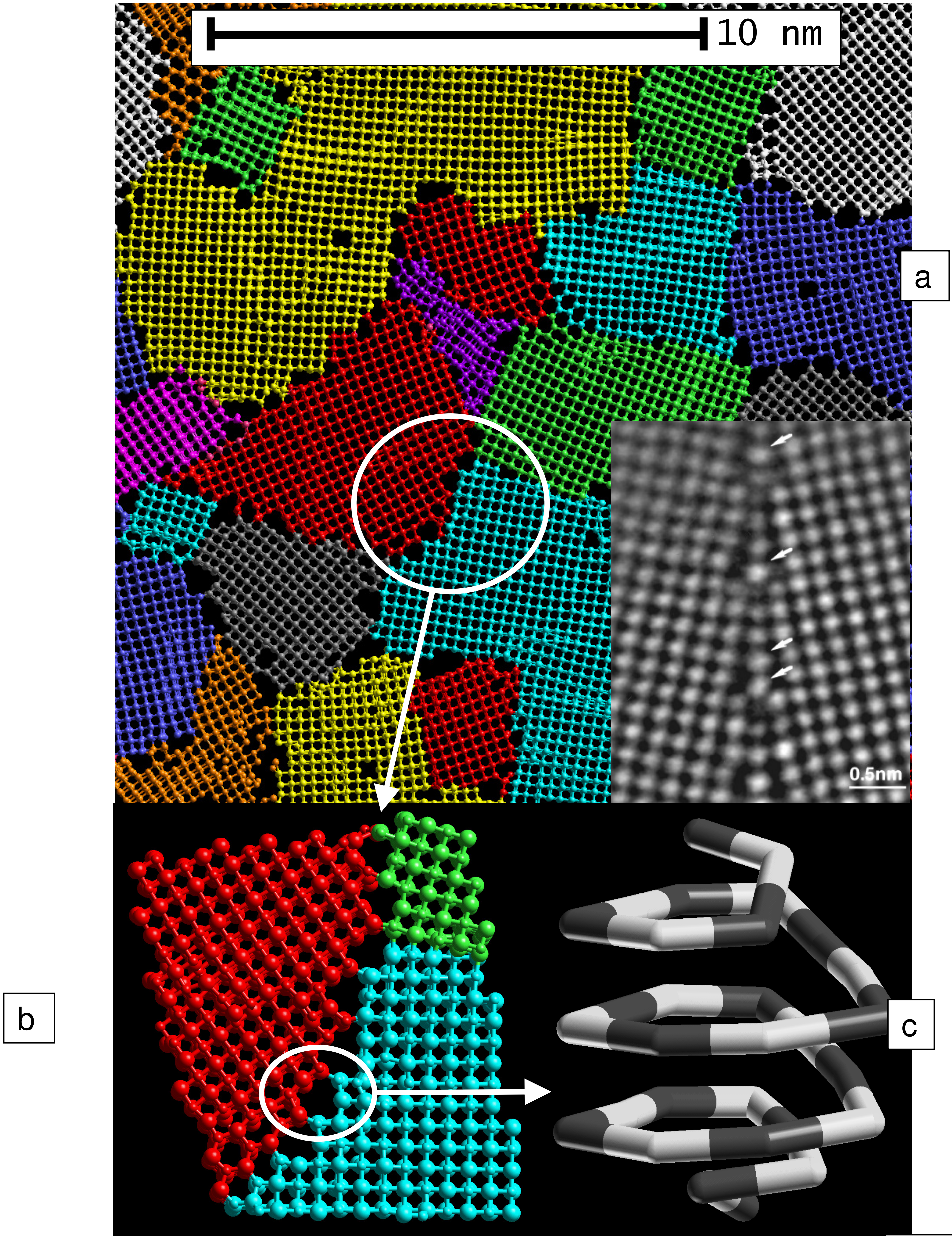

Fig. 9.12

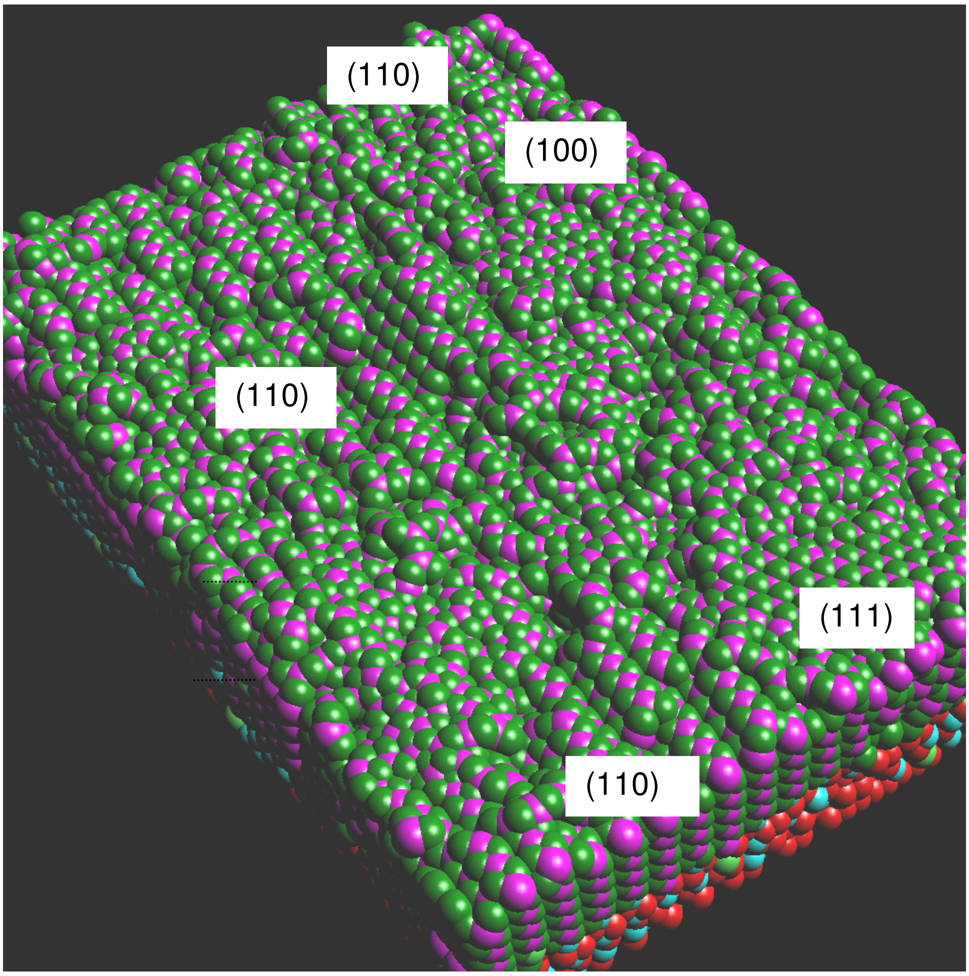
(110)
(100)
(110)
(111)
(110)
a

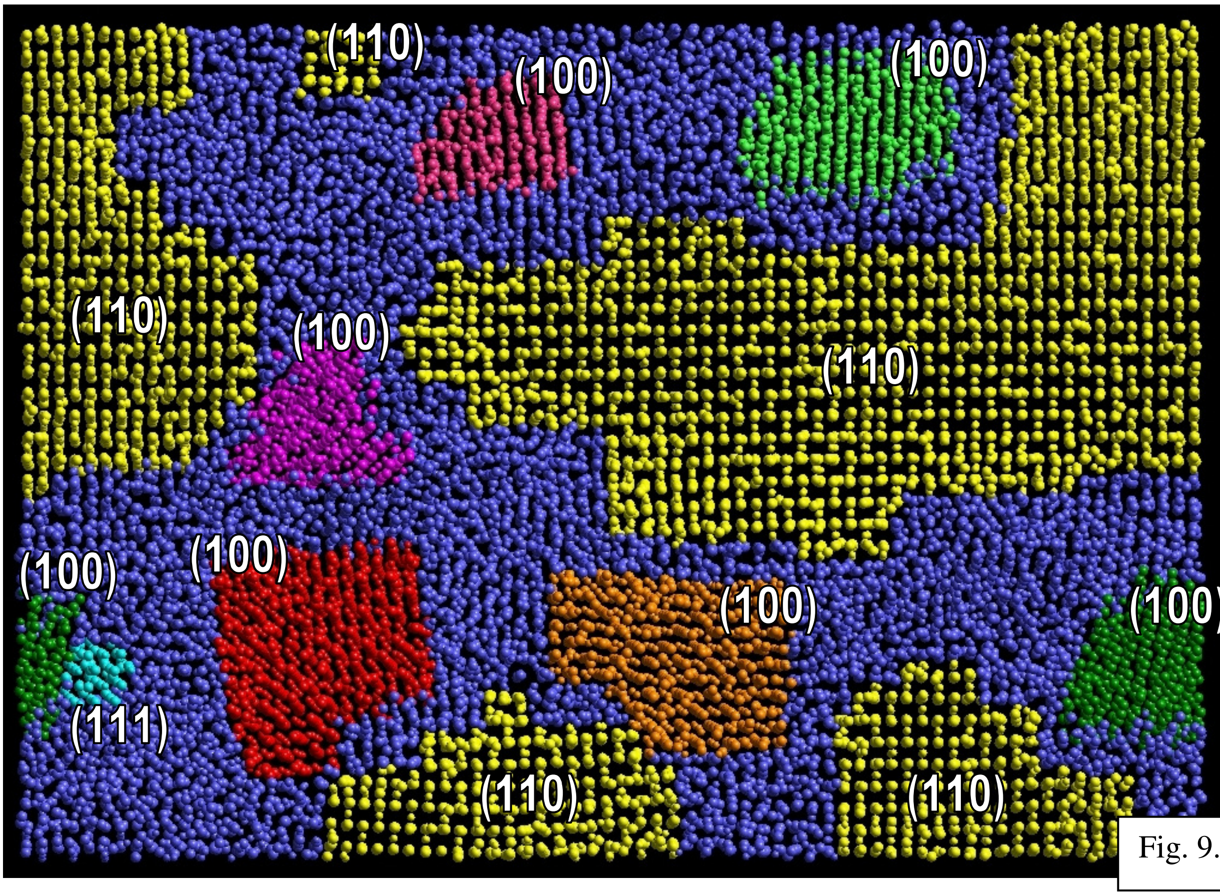
(110)
(100)
(100)
(110)
(100)
(110)
(100)
(100)
(100)
(100)
(111)
(110)
(110)
b

Fig. 9.13

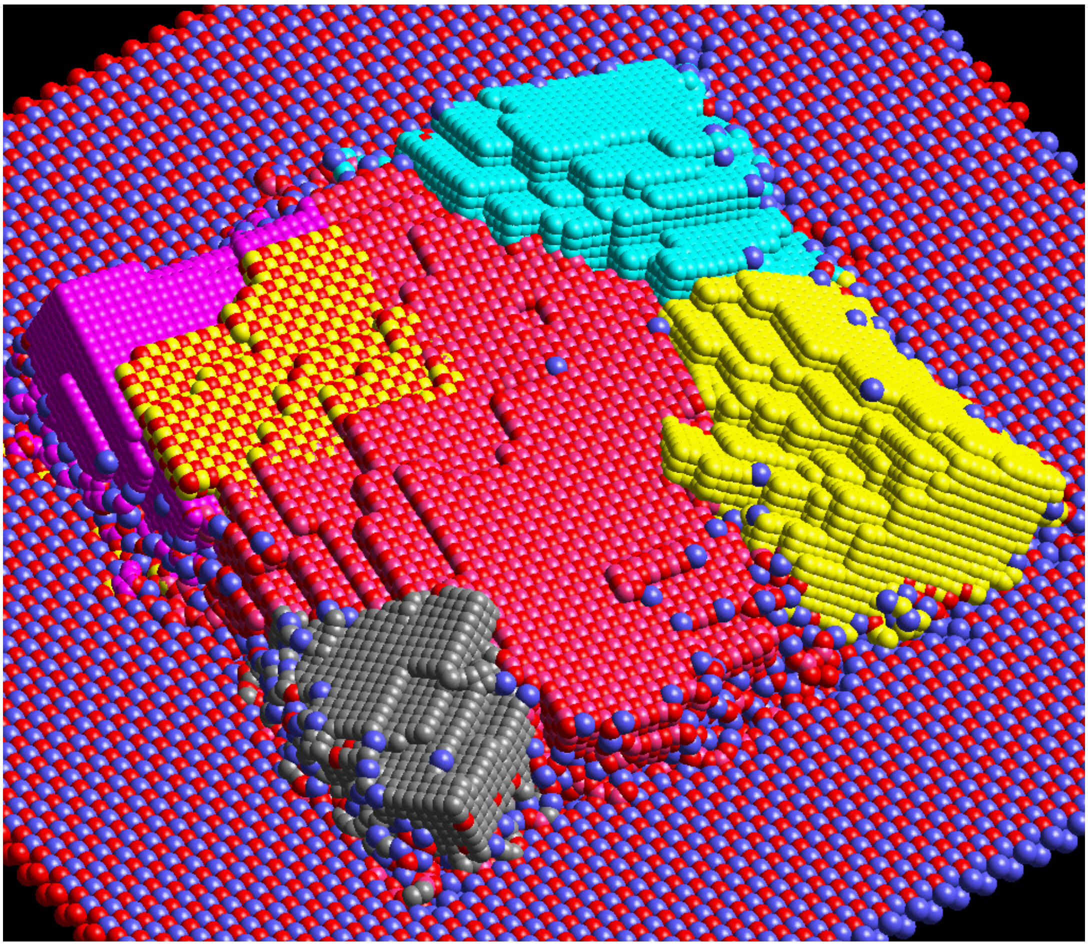

a

b

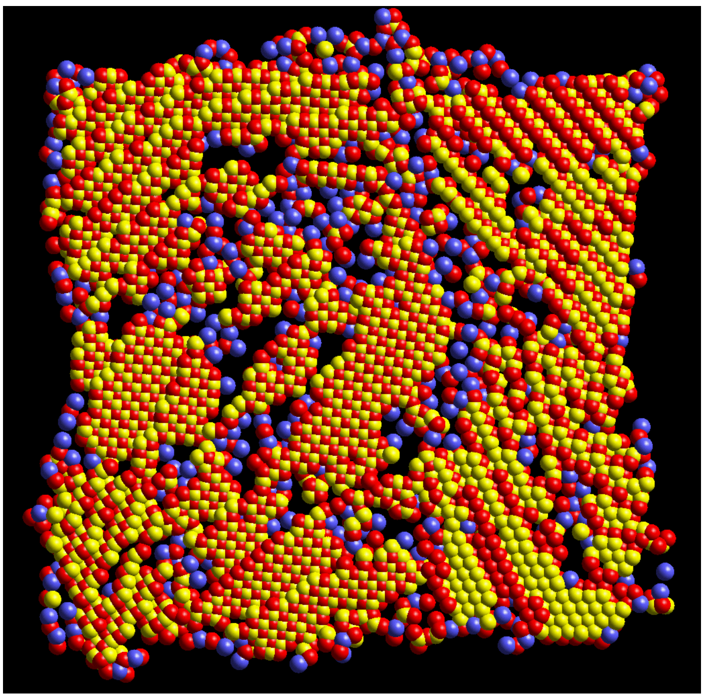

c

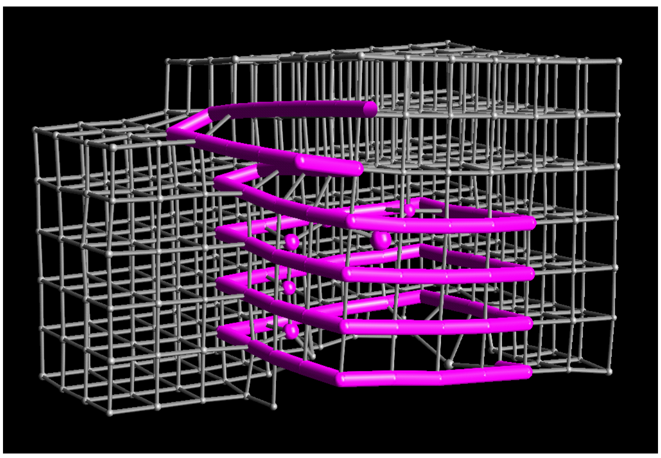

Fig. 9.14

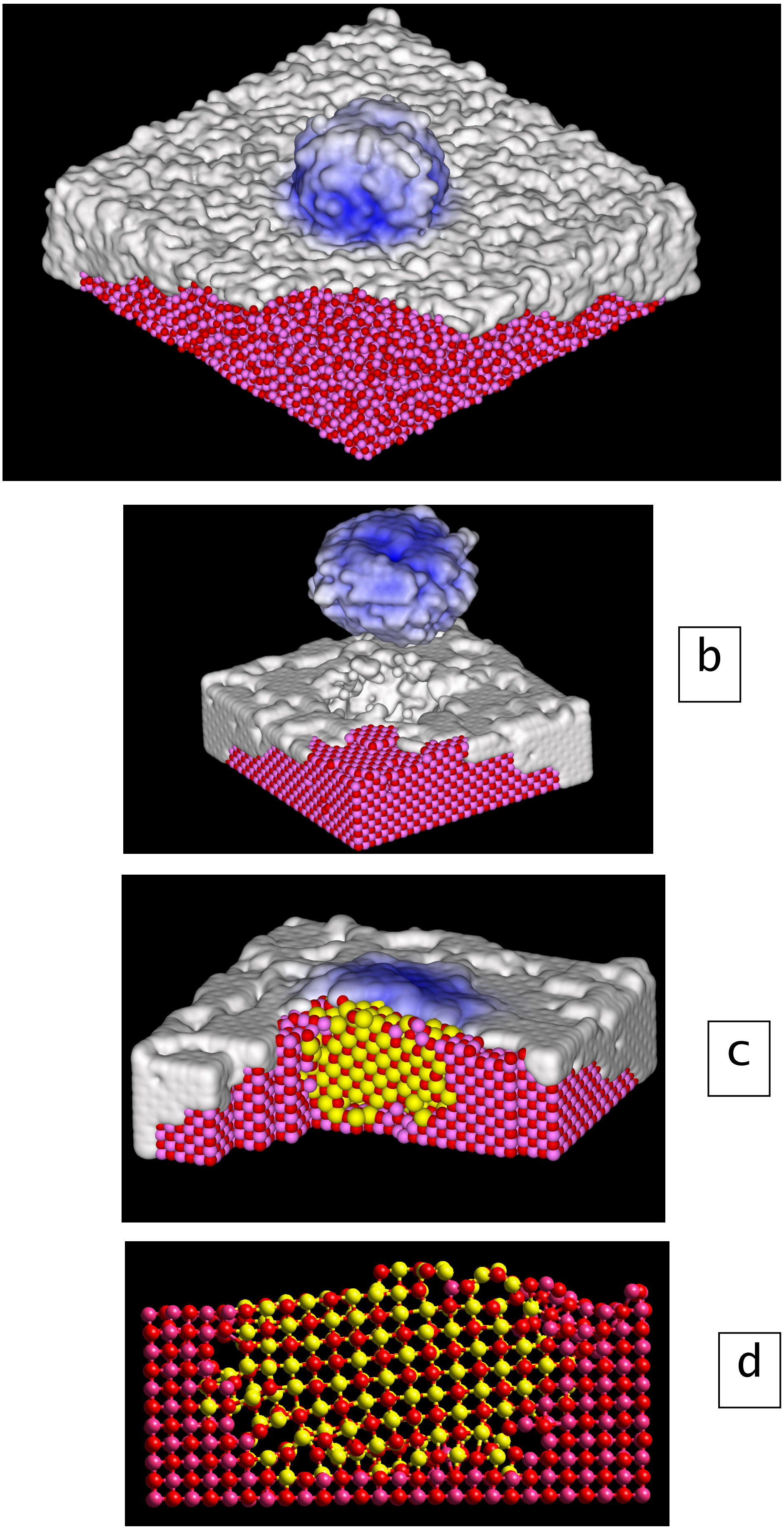

Fig. 9.15

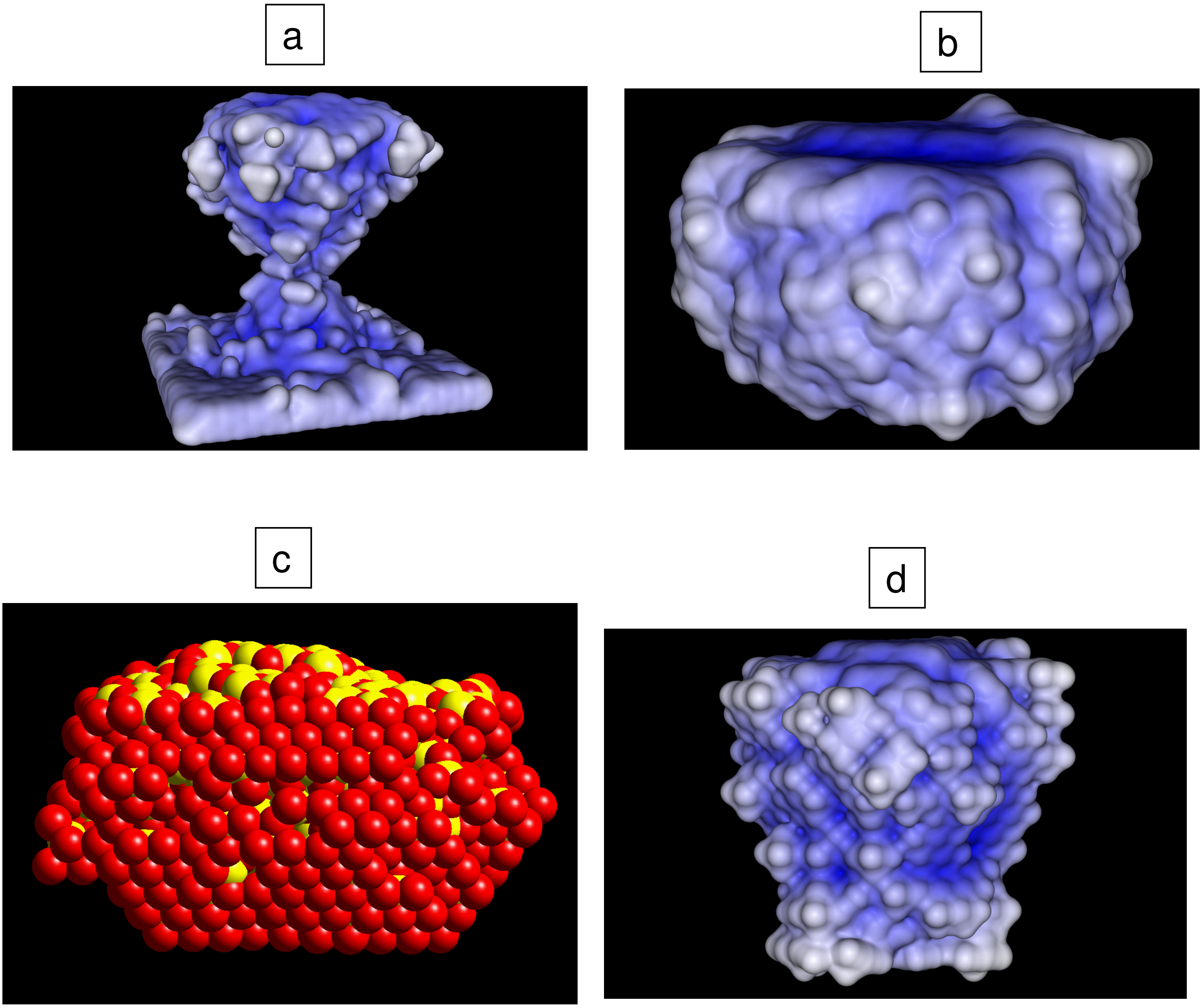

Fig. 9.16

Figure Captions

Figure 9.1 Energy of a diatomic molecule, calculated as a function of interionic separation (r). The force acting upon the ions at any particular interatomic separation can be determined by calculating the gradient (illustrated in the inset).

Figure 9.2 Atom positions corresponding to (a) the starting structure and (b) the amorphous configuration (after 500ps of MD simulation) of the MnO_2 nanoparticle. A sphere model representation of the atoms position has been used. In (b), the atoms comprising the top half of the sphere are represented using a smaller sphere radius to show more clearly the amorphicity of the nanoparticle. Manganese ions are coloured grey and oxygen is red. Some of the ions are coloured yellow to show more clearly that the nanoparticle is spherical.

B/W Manganese ions are light grey and oxygen is dark grey. Some of the ions are coloured white to show more clearly that the nanoparticle is spherical.

Figure 9.3 Snap shots, taken at various time intervals, of a slice cut through the MnO_2 nanoparticle depicting the recrystallisation: (a) after 50ps of MD simulation; (b) after 1150ps; (c) after 1200ps; (d) after 1350ps; (e) after 1600ps; (f) after 4000ps. The energy of the system (10^6 eV), calculated as a function of time, is shown in (g) and can be usefully correlated with the structures (a-f).

Figure 9.4 Structure of the fully recrystallised MnO_2 nanoparticle: (a) sphere model representation of the atom positions. Two different sphere radii have been used for the atoms to aid understanding of the figure; A slice cut through this figure (blue rectangle) is shown in plan view in (b), which depicts the microtwinning of the MnO_2. An enlarged segment is shown in (c). Notation: (a) Manganese atoms are coloured grey and Oxygen, red; (b) Manganese are coloured grey and O atoms above the plane of the paper are red, O ions below the plane of the paper are yellow. The Manganese atoms are shown as ball and stick representation to show more clearly the microtwinning; (c) manganese are shown as grey polyhedra indicating the octahedral sites they occupy, Oxygen atoms above the plane of the paper are red, Oxygen ions below the plane of the paper are yellow.

Figure 9.5 (a) Molecular graphics representations of the theoretical models, (b) high resolution transmission electron micrographs for CeO_2 nanoparticles. (a) Graphical representation of the atom positions comprising each nanoparticle. Top: starting configurations, middle: final configurations, bottom: final configurations with surface rendering rather than sphere model representation. Cerium ions are represented by light grey spheres and oxygen the dark grey spheres. (b) HRTEM reproduced with permission from [Wang ZL 2003] Copyright 2003 American Chemical Society.

Figure 9.6 (a) sphere model representations of the atom positions comprising a slice cut through a CeO_2 nanoparticle revealing the atomistic structure of dipolar {100} surfaces. Notice the similarity between this model structure and the experimental TEM in fig. 9.5(b). The arrows indicate the {100} surfaces. (b) enlarged view of the full nanoparticle, showing more clearly the dipolar surface. (c) plan view showing the surface layer as large spheres and the rest of the crystal as smaller spheres and shows clearly the 50% filling by oxygen of the surface atomic layer, which is necessary to quench the dipole.

Figure 9.7 Sphere model representation of the reduced ceria ($CeO_{1.95}$) nanoparticle. (a-c) depict three different views of the same nanoparticle showing the truncated octahedral morphology, similar to that of the unreduced nanoparticle (fig. 9.5). The Ce^{3+} ions are clearly seen to decorate surface steps and edges in addition to plateau regions on {111} and {100}. In (c) the atomistic structure is annotated with lines to show more clearly the surfaces. (d) segment cut from the reduced nanoparticle depicting an oxygen vacancy bound to an adjacent Ce^{3+}. (e) structure of a Ce^{4+} vacancy together with two adjacent oxygen vacancies, which have evolved to quench the charge imbalance associated with the vacancy. (f) a slice, cut through the nanoparticle, showing two complex defect clusters labeled X and Y. X comprises, using Kroger-Vink notation, $[V_{Ce}^{''''},\ 3V_O^{\bullet\bullet}]^{2-}$ and Y is $[V_{Ce}^{''''},\ 2V_O^{\bullet\bullet}]^{0}$. Ce^{4+} is coloured white, Ce^{3+} is green and oxygen is red.

Figure 9.8 Representations of a CeO_2 nanoparticle that comprises two twin grain-boundaries. (a) sphere model representation. (b) surface rendered representation. (c) sphere model representation with the sphere diameters reduced to show more clearly the twin grain boundaries that run through the nanoparticle. Arrows are included to highlight the boundary planes. (d) HRTEM of a CeO_2 nanoparticle showing the twin grain boundary plane to compare with the theoretical models, reproduced with permission from [Wang ZL 2003] Copyright 2003 American Chemical Society.

Figure 9.9 Sphere model representation of the atom positions during the simulated ion deposition of CaO onto MgO(001). (a) at the start of the simulation; (b) after just over 1 monolayer has been deposited; (c) after the deposition of just over 3 monolayers of CaO onto the MgO substrate. Notice the structural changes that occur as the effective number of monolayers deposited increases. Calcium is coloured blue, magnesium is yellow, oxygen (CaO) is green and oxygen (MgO) is red.

Figure 9.10 Sphere model representations of the atom positions comprising the SrO/MgO(001) system simulated using A&R. (a) start of the simulation, (b) after 0.25ps of MD - the SrO overlayers start to buckle under the considerable strain imposed, (c) after 0.75ps of MD – here the SrO overlayer is completely amorphous, (d) final, 0K, structure after the complete recrystallisation of the SrO overlayer. Oxygen is represented by the dark spheres, strontium, the light spheres and magnesium the smaller spheres. Only two layers of the MgO substrate are shown to improve clarity of the figure.

Figure 9.11 Stick model representations of two screw-edge dislocations that evolved within the SrO thin film. (a) left: part of the SrO lattice (grey) which surrounds the dislocation core, right: dislocation core structure. (b) another dislocation, similar to that in (a) but here the core traverses the SrO thin film in a clockwise fashion (as opposed to anticlockwise in (a)). (c) core structure, shown in red, illustrating how the dislocation core 'lies' within the surrounding lattice. Oxygen is coloured red and strontium is yellow.

Figure 9.12 Atom positions comprising a nanopolycrystalline MgO thin film supported on a BaO substrate. (a) Plan view of the system showing the various nanocrystallites comprising the MgO, which are coloured to highlight the individual nanocrystallites. The MgO substrate is not shown to maintain clarity of the figure. The inset shows a STEM image to compare and has been reproduced, with permission, from [Pennycook SJ 1999] Copyright 1999 European Ceramic Society. (b) Enlarged segment of (a) showing more clearly the grain-boundary structure. (c) An enlarged segment of (b) depicting the core structure of the grain-boundary and revealing its 'screw' in addition to 'edge' character.

Figure 9.13 Sphere model representation of the atom positions comprising the CeO_2/YSZ system. (a) perspective view, (b) plan view in which the various nanocrystallites are coloured. The figures are annotated to reveal which particular planes – (111), (110) or (100) - are exposed at the surface.

This can be represented in B/W if necessary with no change to the caption and a relatively small reduction to the scientific content or understanding; clarity would be poor however.

Figure 9.14 (a) Perspective view, with sphere model representations, of the atom positions comprising a 25,000 atom MgO nanoparticle supported on a BaO(001) substrate. The various miss-oriented crystallites are coloured. (b) interfacial region illustrating the considerable defective nature of the interfacial region. (c) mixed screw edge dislocation that was identified to have evolved within the MgO nanoparticle.

Figure 9.15 Representation of the atom position illustrating the encapsulation of a CaO nanoparticle within an MgO host lattice. (a) amorphous starting structure showing the CaO nanoparticle being introduced into the MgO host. (b) final recrystallised structure showing the structure of the CaO nanoparticle and the void in the MgO that it occupies (the CaO nanoparticle has been physically extracted to reveal the structure). (c) perspective view with part of the simulation cell cut-away to reveal the CaO nanoparticle encapsulated by its MgO host. (d) slice cut through the simulation cell to reveal more clearly how the CaO nanoparticle lies with respect to the host. Calcium is coloured yellow, oxygen is red and magnesium is purple. Surface rendering has also been used to aid interpretation of the structures. White rendering is the MgO host and white-blue, the CaO nanoparticle.

B/W Calcium is coloured light grey, magnesium is medium grey and oxygen dark grey. Surface rendering has also been used to aid interpretation of the structures. Light grey rendering is the MgO host and light/dark rendering, the CaO nanoparticle.

B/W makes only a slight change to the scientific understanding; the clarity would be poor.

Figure 9.16 Representations of the atom positions of oxide nanoparticles (shown) encapsulated within an oxide host lattice (not shown). (a) MgO nanoparticle (in BaO host), (b) BaO nanoparticle (in MgO host), (c) CaO nanoparticle (in MgO host), (d) SrO nanoparticle (in BaO host). a, b and d are shown with surface rendering and b using a sphere model representation of the atom positions.

Table captions

Table 9.1 Calculated energies associated with oxidising CO to CO_2 using lattice oxygen from CeO_2. Energies are calculated in eV. For the nanoparticle, the energy is an average (equation 9.9) calculated over all the defects. *taken from ref. [Sayle TXT 1992].

Bulk*	(111)*	(110)*	(310)*	Nanoparticle
3.1	- 0.6	- 2.8	-1.9	- 1.4